Research Square

Preprints are preliminary reports that have not undergone peer review.
They should not be considered conclusive, used to inform clinical practice,
or referenced by the media as validated information.

Transcriptome analysis of Bacillus licheniformis M2-7 reveals metabolic pathways involved in gasoline oxidation

Augusto Rojas-Aparicio
Universidad Autónoma de Guerrero
Mariana Reyes-Prieto
Fundación para el Fomento de la Investigación Sanitaria y Biomédica de la Comunitat Valenciana
Alberto Hernández-Eligio
Universidad Nacional Autónoma de México
Jeiry Toribio-Jiménez
Universidad Autónoma de Guerrero
Yanet Romero-Ramírez
yanetromero7@gmail.com

Universidad Autónoma de Guerrero

Research Article

Keywords: Bacillus licheniformis M2-7, gasoline, metabolic pathways, oxidation, transcriptome

Posted Date: November 20th, 2026

DOI: https://doi.org/10.21203/rs.3.rs-10349766/v1

License: This work is licensed under a Creative Commons Attribution 4.0 International License.
Read Full License

Additional Declarations:
No competing interests reported.

One or more figures are unavailable with this version.

Transcriptome analysis of *Bacillus licheniformis* M2-7 reveals metabolic pathways involved in gasoline oxidation

Augusto Rojas-Aparicio[1], https://orcid.org/0009-0004-4269-4589

Mariana Reyes-Prieto[2], https://orcid.org/0000-0001-6292-2420

Alberto Hernández-Eligio[3,4], https://orcid.org/0000-0002-2787-8732

Jeiry Toribio-Jiménez[1], https://orcid.org/0000-0002-9455-6442

Yanet Romero-Ramírez[1*], https://orcid.org/0000-0002-8383-4128

[1]Laboratorio de Microbiología Molecular y Biotecnología Ambiental, Facultad de Ciencias Químicas y Biológicas, Universidad Autónoma de Guerrero, Avenida Lázaro Cárdenas, Ciudad Universitaria, 39070, Chilpancingo, Guerrero, México.

[2]Unidad de Servicios de Investigación de la Fundación para la Promoción de la Salud y la Investigación Biomédica de la Comunidad Valenciana (FISABIO), Salud Pública de la Generalitat Valenciana. Avenida de Cataluña, 21, Benimaclet, 46020, Valencia, España.

[3]Departamento de Microbiología Molecular, Instituto de Biotecnología, Universidad Nacional Autónoma de México. Avenida Universidad, 2001, Chamilpa, 62210, Cuernavaca, Morelos, México.

[4]Secretaría de Ciencia, Humanidades, Tecnología e Innovación. Avenida Insurgentes Sur, 1582, Benito Juárez, 0394, Ciudad de México, México.

*Corresponding author. E-mail: yanetromero7@gmail.com

Abstract

Bacillus licheniformis M2-7 is a bacterium capable of using gasoline as a carbon source. However, the molecular mechanisms underlying this process remain unknown. Therefore, this study sought to elucidate the global metabolic pathways involved in gasoline degradation by this bacterium. Transcriptomic analysis of *Bacillus licheniformis* M2-7 was conducted after 3 h of incubation in medium supplemented with either 0.1% gasoline or 2% glucose. RNA samples were extracted, purified, quantified, chemically fragmented, and used for cDNA library synthesis. The libraries were sequenced using an Illumina platform. Sequence quality control was performed, the reads were assembled, the sequences were then mapped, and differential gene expression analysis was carried out. Functional annotation and reconstruction of degradation pathways were also performed. To validate the RNA-seq results, qPCR analysis was conducted on 17 genes under gasoline oxidation conditions. In addition, the motility and biosurfactant production were experimentally confirmed. A total of 2,660 genes were differentially expressed (1,340 upregulated and 1,320 downregulated). Functional analysis of the response of M2-7 strain to gasoline oxidation revealed 67 enrichment pathways. The most strongly affected pathways were associated with quorum-sensing, two-component systems, and others. Furthermore, at least 40 genes potentially involved in gasoline metabolism were identified. The expression of genes encoding oxygenases, dehydrogenases, oxidoreductases, and hypothetical proteins were validated. The results also showed that the bacterium exhibits gliding motility and produces 1,166 mg/L of biosurfactants. Overall, this study provides new insights into the mechanisms of gasoline degradation by *Bacillus licheniformis* M2-7 and supports its potential application in bioremediation processes.

Keywords: *Bacillus licheniformis* M2-7, gasoline, metabolic pathways, oxidation, transcriptome.

Introduction

Gasoline is a refined petroleum product composed of a complex mixture of hydrocarbons, including alkanes, alkenes, isoalkanes, cycloalkanes, cycloalkenes, and aromatic compounds (IARC 1989; Conceição et al. 2019). Pollution caused by gasoline combustion and accidental spills has affected aquatic, atmospheric, and terrestrial environments and is considered a major threat to ecosystem health (WHO 2010). Various physical and chemical approaches have been developed to remediate gasoline spills and contamination by its components, with the aim of minimizing their environmental impact (Khan, Husain, and Hejazi 2004; Venny-Gan and Ng 2012; Silva-Castro et al. 2013). Among these strategies, biological treatments have proven to be highly effective. In particular, bioremediation using native soil

microorganisms takes advantage of both *in situ* and *ex situ* applications for the treatment of gasoline-contaminated sites (Silva-Castro et al. 2013; Khayati and Barati 2017; Elenga-Wilson et al. 2021). These approaches offer several advantages, including low energy requirements, reduced operating costs, the absence of secondary pollutants, and the rapid recovery of soil functionality (Ugochukwu, Manning and Fialips 2014; Sarkar et al. 2016; Prosser et al. 2016; Gupta et al. 2018).

Although bacterial genera have been reported to degrade hydrocarbons, relatively few are capable of degrading gasoline because of its complex composition. Reported gasoline-degrading genera include *Gordonia*, *Pseudomonas*, *Dietzia*, *Microbacterium*, *Mycobacterium*, and *Bacillus* (Ángel et al. 2020; Baburam and Feto 2021; Frantsuzova et al. 2023; Goma-Tchimbakala et al. 2023). These bacteria exploit their enzymatic potential to degrade hydrocarbons through both aerobic and anaerobic pathways (Zhang, Hu, and Wang 2019; Solís-González and Loza-Tavera 2019; Guevara-Luna et al. 2022; Goma-Tchimbakala et al. 2023). Hydrocarbon degradation depends on the chemical complexity and toxicity of the compounds involved, with high-molecular-weight polycyclic aromatic hydrocarbons (PAHs) considered particularly toxic (US EPA 1979; Zhang, Davis and Erickson 1998; Lico et al. 2019). In *Bacillus subtilis*, *Bacillus mojavensis*, and *Bacillus licheniformis*, aerobic degradation of PAHs involves multicomponent dioxygenases, reductases, ferredoxins, and other proteins that catalyze ring cleavage reactions and ultimately generate intermediates that enter the tricarboxylic acid cycle (Fuchs 1999; Izquierdo 2013; Eskandari et al. 2017; Ángel et al. 2020; Guevara-Luna et al. 2022). The participation of cytochrome P450 monooxygenases has also been reported (Heitkamp et al. 1988a, b; Kelley, Freeman, and Cerniglia 1990; Izquierdo 2013). Degradation pathways for a wide range of aromatic compounds converge through the formation of a limited number of monoaromatic intermediates, primarily catechol and protocatechuate or their methylated derivatives. These intermediates are subsequently converted into central metabolites that enter the tricarboxylic acid cycle or are utilized in the biosynthesis of other cellular components (Fuchs 1999; Izquierdo 2013).

In addition, hydrocarbon-degrading bacteria may produce biosurfactants that reduce surface tension at the water-oil interface, thereby increasing the bioavailability of hydrophobic contaminants (Mata-Sandoval et al. 1999; Abalos et al. 2001; Stancu 2020; Zambry et al. 2021; Okeke et al. 2022). *B. licheniformis* M2-7 is a thermoresistant bacterium isolated from hot springs (Guevara-Luna et al. 2022). This hydrocarbonoclastic strain is capable of metabolizing a variety of hydrocarbons, including crude oil and gasoline, as well as potentially toxic compounds such as anthracene, benzene, xylene, and benzo[a]pyrene (BaP) (Rojas-

Aparicio et al. 2018; Guevara-Luna et al. 2018; Guevara-Luna et al. 2022). Furthermore, the expression of catechol-2,3-dioxygenase and genes encoding 4-hydroxybenzoate-3-monooxygenase and ketoacyl-ACP synthase III was previously detected after 3 h of exposure to BaP (Rojas-Aparicio et al. 2018; Guevara-Luna et al. 2022). Although these findings suggest that *B. licheniformis* M2-7 has considerable potential for bioremediation applications, the molecular basis of gasoline degradation remains poorly understood. Recent advances in transcriptomics have provided valuable insights into the metabolic responses of different bacterial genera and have contributed to the elucidation of the global pathways involved in hydrocarbon degradation (Zhang, Hu, and Wang 2019; Goma-Tchimbakala et al. 2023). For example, the transcriptional profile of *Pseudomonas aeruginosa* ATCC 33988 grown in fuel revealed 3,580 differentially expressed genes (DEGs), including 2,963 upregulated and 617 downregulated genes associated with alkane degradation, heat-shock response, membrane proteins, and efflux pumps (Gunasekera et al. 2013). Similarly, *Achromobacter* sp. HZ01 grown in petroleum-containing medium exhibited 742 DEGs, of which 278 were upregulated and 464 were downregulated. In this strain, monooxygenases, dehydrogenases, and fatty acid metabolism were activated, whereas the tricarboxylic acid cycle remained inactive (Hong et al. 2016). *Lysinibacillus fusiformis* 15-4 differentially expressed 2,192 genes during growth in petroleum-containing medium, including 1,312 upregulated and 880 downregulated genes (Li, Huang, and Liu 2020). Likewise, *P. aeruginosa* strains N002, TP16, and J001 exposed to crude oil showed differential expression of 81, 269, and 137 genes, respectively, mainly involved in carbohydrate metabolism, transmembrane transport, transcription factor activity, and oxidoreductase activity (Das et al. 2020). However, the regulatory networks and degradation pathways involved in gasoline metabolism by *B. licheniformis* have not yet been comprehensively characterized. Therefore, the aim of this study was to elucidate the global mechanisms underlying gasoline degradation in *B. licheniformis* M2-7 through transcriptomic analysis and to provide a metabolic framework for understanding this process.

Materials & Methods

Bacteria and cell cultures

B. licheniformis M2-7, obtained from the collection of the Laboratorio de Microbiología Molecular y Biotecnología Ambiental at the Universidad Autónoma de Guerrero, was used in this study. Strain M2-7 was cultivated in Luria-Bertani (LB) liquid medium containing 10.0 g/L casein peptone, 5.0 g/L yeast extract, and 10.0 g/L NaCl (pH 7.3). Cultures were incubated at 37 °C with shaking at 180 rpm for 24 h. For the gasoline oxidation assay, a minimal salt medium (MSM) modified from Zeinali et al. (2008) was

used. The MSM composition was as follows (g/L): NH_4Cl, 1.0; Na_2HPO_4, 0.380; $KH_2PO_4 \cdot H_2O$, 0.380; $MgSO_4 \cdot 6H_2O$, 0.080; $CaCl_2$, 0.070; KCl, 0.040; and $FeSO_4 \cdot 7H_2O$, 0.001. A trace element solution (2.5 mL/L medium) containing the following components (g/L) was added: $MgCl_2 \cdot 4H_2O$, 0.027; H_3BO_3, 0.031; $ZnCl_2$, 0.050; $CuCl_2 \cdot 2H_2O$, 0.01; $NiCl_2 \cdot 6H_2O$, 0.02; $CoCl_2 \cdot 6H_2O$, 0.036; and $Na_2MoO_4 \cdot 2H_2O$, 0.03. The medium was adjusted to pH 7.0 and supplemented with either 0.1% gasoline or 2% glucose. Degradation experiments were carried out at 37 °C for 3 h.

RNA extraction and RNA-seq analysis

All experiments were performed in triplicate using independent biological samples. Cells of *B. licheniformis* M2-7 were harvested from MSM cultures after 3 h of incubation. The control group consisted of cells grown in MSM supplemented with 2% glucose (Control_S1_1, Control_S1_2, and Control_S1_3), whereas the experimental group consisted of cells grown in MSM supplemented with 0.1% gasoline (Bac_Gaso_S2_1, Bac_Gaso_S2_2, and Bac_Gaso_S2_3). Total RNA was extracted from each biological sample using the RNeasy Mini Kit (Qiagen) according to the manufacturer's instructions. RNA quality was evaluated using an Agilent 2100 Bioanalyzer, and RNA purity and concentration were determined using a NanoDrop 2000c spectrophotometer (Thermo Scientific). Contaminating DNA was removed with DNase I (RNase-free) (Thermo Scientific). Illumina sequencing was performed at the University Unit of Massive Sequencing and Bioinformatics (UUSMB, UNAM, Mexico). Ribosomal RNA was removed using the RiboMinus Kit (Thermo Scientific), and the enriched RNA was chemically fragmented into 150–200 bp fragments. cDNA libraries were constructed using the TruSeq Stranded mRNA Kit (Illumina) and purified using the ZymoClean Gel DNA Recovery Kit (Zymo Research). Sequencing was performed on an Illumina NextSeq 500 platform.

Quality control and sequence alignment

RNA-seq sequence quality analysis was performed using the Fastp (v0.22.0, Chen 2023). To assemble the sequences, the program FLASH (v1.2.11, Magoč and Salzberg 2011) was used, once the overlapping sequences were obtained, the next step consisted of a de *novo assembly* of the transcripts using the rnaSPAdes software (v3.13.1, Prjibelski et al. 2020). The *contigs* were then used to perform a BLAST-NCBI, obtained that the taxonomically similar reference genome is *Bacillus licheniformis* strain DSM13 (99.84% identity) accession code CP093290.1. We used BWA (v.0.7.17-r1188, Li and Durbin 2010) to map the sequences with the reference genome through alignments. SAMtools (v1.13, Danecek et al. 2021) was also used to transform short-read DNA sequence alignments from SAM to BAM formats. Both programs

allow the creation of a series of data related to alignments, classification, indexing, data extraction, and format conversion.

Differential gene expression analysis

DEGs were identified using Cuffdiff (v2.2; Trapnell et al. 2012) and DESeq2 (Anders and Huber 2010). Genes with a p-value ≤ 0.05 and a fold change ≥ 2 were considered differentially expressed. The analysis pipeline was automated using the NF-Core/DifferentialAbundance platform (v1.2.0, Ewels et al. 2020) to ensure reproducibility. Functional annotation and pathway analysis of differentially expressed genes were performed using the Kyoto Encyclopedia of Genes and Genomes (KEGG) database (Kanehisa and Goto 2000) with custom R scripts. RNA-seq data were deposited in the NCBI Gene Expression Omnibus database under accession number GSE337535.

Quantitative real-time PCR (RT-qPCR)

To validate the RNA-seq results, RT-qPCR analysis was performed on 16 DEGs. Nine genes were upregulated (*acoC, yxlF, fadE2, ykvT*, BLi01956, *yhjG, mhqO, yrbE*, and *ythA*), whereas seven genes were downregulated (*spoVG, lchAA, scdA*, *gapA, fabH2, nasD,* and *degQ*). Primer pairs for each gene were previously evaluated for specific amplification by endpoint PCR using genomic DNA. RNA extraction and purification were performed as described above. cDNA was synthesized using the RevertAid H Minus First Strand cDNA Synthesis Kit (Thermo Scientific) with 1 µg of DNase-treated RNA and 20 pmol of gene-specific reverse primers (Supplementary Table 1). Quantitative PCR was performed using Maxima SYBR Green qPCR Master Mix (Thermo Scientific) in a Rotor-Gene Q system (Qiagen). The thermal cycling conditions consisted of an initial denaturation step at 95 °C for 10 min, followed by 40 cycles of 95 °C for 15 s and 60 °C for 60 s. The *rpoB* gene was used as the internal reference, and relative gene expression levels were calculated using the $2^{-\Delta\Delta CT}$ method (Livak and Schmittgen, 2001).

Confirmation of motility and biosurfactant production

Mobility phenotype

A total of 1×10^6 cells of *B. licheniformis* M2-7 were inoculated into MSM containing 7 g/L bacteriological agar and supplemented with either 2% glucose (control) or 0.1% gasoline (treatment). Cultures were incubated at 37 °C for 24–48 h. Motility assays were performed in triplicate, and the diameters of the motility zones were measured and compared between treatments.

Biosurfactant production assay

Biosurfactant extraction and quantification were performed according to the method described by Sun et al. (2018). Briefly, 1×10^8 cells of *B. licheniformis* M2-7 were inoculated into Bushnell-Haas medium containing (g/L): NH_4NO_3, 1.0; $KH_2PO_4 \cdot H_2O$, 1.0; $K_2HPO_4 \cdot H_2O$, 1.0; $MgSO_4 \cdot 7H_2O$, 0.2; $FeCl_2$, 0.05; and $CaCl_2 \cdot 2H_2O$, 0.02. The medium was supplemented with either 2% glucose or 0.1% gasoline and adjusted to pH 7.0. Cultures were incubated for 96 h, after which they were centrifuged at 7,000 rpm and 4 °C for 20 min. The supernatant was acidified to pH 2 with 6 N HCl and stored at 4 °C for 16 h. Samples were centrifuged again, and an equal volume of chloroform (2:1) was added to the supernatant. This extraction step was repeated twice. The organic phase was collected, and the biosurfactant was weighed after solvent evaporation.

Statistical analysis

RT-qPCR data were analyzed by one-way analysis of variance (ANOVA), followed by Tukey's multiple comparison test. Differences were considered statistically significant at $p < 0.05$. Motility and biosurfactant production data were analyzed using Student's t-test. All statistical analyses were performed using GraphPad Prism version 7 (GraphPad Software, Inc.).

Results

Based on previous studies showing that *B. licheniformis* M2-7 can grow with gasoline as its sole carbon source (Ángel et al. 2020) and biotransform BaP into phthalic acid within 3 h of incubation (Guevara-Luna et al. 2018), this time point was selected for RNA extraction and transcriptomic profiling. Quality control of the RNA-seq libraries confirmed fragment sizes of approximately 150 bp and yielded an average of 24–27 million paired-end reads per sample, with Q30 quality scores consistently exceeding 96% (Fig. 1A). Exploratory analyses (Fig. 1B and C) revealed clear differences between cells grown with glucose as the carbon source (Control_S1_1, S1_2, and S1_3) and those exposed to gasoline (Bac_Gaso_S2_1, S2_2, and S2_3). In addition, high similarity was observed among the biological replicates within each treatment group. Principal component analysis (PCA) of the RNA-seq data (Fig. 1D) showed a clear separation between gasoline-treated samples and controls. However, one sample (Bac_Gaso_S2_1) was separated from the other two gasoline-treated replicates, indicating greater variability within this group. The data were subsequently adjusted to account for this variation and to enable differential expression analysis.

Differential expression analysis identified 1,320 upregulated genes and 1,340 downregulated genes among the 4,048 annotated ORFs in gasoline-treated cultures compared with the control condition (Fig. 2). These

transcriptional changes indicate extensive metabolic reprogramming, affecting approximately 50% of the *B. licheniformis* genome in response to gasoline exposure.

Transcriptomic analysis revealed a substantial number of DEGs associated with the degradation of petroleum hydrocarbons, diesel, gasoline, and PAHs, as well as with biosurfactant production (Table 1). Among the thirteen oxygenase-related enzymes identified, seven were differentially expressed, including the monooxygenase YcnE, catechol-2,3-dioxygenase CatE, aliphatic sulfonate monooxygenase SsuD, dioxygenase MhqA, dioxygenase MtnD, putative aromatic monooxygenase YhjG, and putative ring-cleaving dioxygenase MhqO. In addition, genes encoding acetoin dehydrogenase (AcoC), transketolase, cytochrome d, and at least eleven putative enzymes were upregulated.

To predict the functional response of *B. licheniformis* M2-7 to gasoline catabolism, DEGs were subjected to enrichment analysis using KEGG and KEGG Orthology. The analysis revealed 67 significantly enriched pathways ($p < 0.05$) with altered gene expression. Fig. 3 presents the representative pathways containing the largest numbers of DEGs, including amino acid biosynthesis (100 DEGs), cofactor biosynthesis (100 DEGs), the two-component system (98 DEGs), carbon metabolism (79 DEGs), quorum sensing (58 DEGs), flagellar assembly (35 DEGs), and oxidative phosphorylation (30 DEGs). Among these pathways, genes involved in flagellar assembly showed pronounced differential expression, with 25 upregulated genes and 10 downregulated genes. In particular, genes belonging to the flagellar biosynthesis operons (*fliZ*, *fliP*, *fliQ*, *fliR*, *flhB*, *flhA*, *flhF*, and *ylxH*) and those encoding flagellar basal-body rod proteins (*flgB*, *flgC*, *flgF*, and *flgG*) were consistently upregulated. Another pathway showing extensive transcriptional changes was the two-component system, which comprised 55 upregulated genes and 44 downregulated genes. These results suggest activation of oxygen-responsive genes and membrane-associated proteins, whereas genes involved in sporulation appear to be repressed. Changes were also observed in quorum sensing, with 25 upregulated genes and 33 downregulated genes. Notably, the *lichAA*, *lichAB*, *lichAC*, and *lichAD* genes, which encode the lichenysin synthase complex, were upregulated, exhibiting fold changes of 1.20, 1.60, 1.47, and 0.47, respectively.

Other DEGs associated with transport processes, lipid, carbohydrate, and amino acid metabolism, transcriptional regulation, and the repression of protein synthesis-related functions, including ribosomal proteins, translation, and post-translational modifications, were also identified. These findings provide a foundation for a more comprehensive understanding of gasoline component utilization and the metabolic pathways involved.

To validate the RNA-seq results and obtain quantitative measurements of transcript abundance under gasoline oxidation conditions, RT-qPCR analysis was performed on 16 selected genes (9 upregulated and 7 downregulated) involved in the degradation of major gasoline components, transcriptional regulation, and central metabolism (Table 2). Among the upregulated genes were those encoding oxygenase and dioxygenase enzymes, including the putative aromatic monooxygenase YhjG (*yhjG*) and the putative ring-cleaving dioxygenase MhqO (*mhqO*). Additional genes encoded the ATP-binding ABC-type antimicrobial peptide transporter protein YxlF (*yxlF*), two dehydrogenases, acetoin dehydrogenase (*acoC*) and acyl-CoA dehydrogenase (*fadE*), the cytochrome bd ubiquinol oxidase subunit I (*ythA*), and the putative NAD(P)-dependent oxidoreductase YrbE (*yrbE*). Two other genes encoded a transmembrane protein (BLi04328) and a hypothetical protein (BLi01956), both of which remain uncharacterized.

The high expression levels of *yxlF*, *fadE2*, *vkyT*, *yhjG*, *mhqO*, *yrbE,* and *ythA*, as well as a hypothetical protein (BLi01956), were confirmed in *B. licheniformis* M2-7 grown in the presence of gasoline (Table 2). Conversely, downregulation was observed for genes encoding the putative septation protein SpoVG, lichenysin synthase LchAA, regulator ScdA, glyceraldehyde-3-phosphate dehydrogenase 1, beta-ketoacyl-acyl carrier protein synthase, assimilatory nitrite reductase, and the pleiotropic regulator DegQ. The expression patterns determined by RT-qPCR were consistent with those obtained by RNA-seq, supporting the reliability of the transcriptomic data.

To further verify the transcriptional changes observed during gasoline oxidation, bacterial motility was evaluated under the same conditions. As shown in Fig. 4, significant differences in motility were detected between control and gasoline-treated cultures ($P = 0.0293$). Reduced motility was observed in the presence of gasoline, suggesting that exposure to gasoline imposes physiological stress on the cells. In *Bacillus* species, *sliding* motility, a non-flagellar form of surface translocation, is closely associated with biosurfactant production. By reducing surface tension, biosurfactants facilitate bacterial movement toward nutrient-rich regions and may also help cells avoid unfavorable conditions caused by hydrocarbon toxicity.

Another phenotype evaluated under gasoline oxidation conditions was biosurfactant production. Biosurfactant concentrations were quantified, yielding average values of 1,861 mg/L for the control and 1,028 mg/L for the gasoline treatment (Fig. 5). Statistically significant differences were observed among the treatments, indicating that *B. licheniformis* M2-7 preferentially utilizes simple carbon sources such as glucose. Nevertheless, the strain retained the ability to produce biosurfactants in the presence of gasoline, albeit at substantially lower levels than those observed in the control cultures.

It is worth noting that both of the evaluated phenotypes (motility and biosurfactant production) were assessed after prolonged incubation periods (48 h and 96 h, respectively). Both phenotypes exhibited changes under these conditions, indicating that the physiological responses observed at these later points differed from those detected by RNA-seq, which was performed after only 3 h of exposure to gasoline.

Discussion

This study proposes a model for the degradation pathways involved in the metabolism of gasoline components by *B. licheniformis* M2-7, highlighting its considerable metabolic versatility. Previous studies have shown that this strain can utilize a wide range of hydrocarbons, from complex mixtures such as gasoline and diesel to low-molecular-weight PAHs, including phenanthrene, pyrene, and anthracene, as well as high-molecular-weight PAHs such as BaP (Guevara-Luna et al. 2018; Guevara-Luna et al. 2022). The ability of strain M2-7 to biotransform BaP into phthalic acid has also been reported, supporting its potential application in combined biodegradation strategies (Guevara-Luna et al. 2018). Understanding the microbial degradation of hydrocarbons remains an important area of research because of its implications for the development of effective bioremediation approaches (Agnez-Lima, Vainstein, and Zhang 2024).

Among hydrocarbon-degrading bacteria, *Pseudomonas aeruginosa* is one of the most extensively studied species, particularly regarding the oxidation of aromatic compounds through monooxygenase- and dioxygenase-mediated pathways (Gunasekera et al. 2013; Das et al. 2020). Three major pathways for aliphatic hydrocarbon degradation have been described: (1) the monoterminal pathway, in which terminal methyl groups are oxidized to fatty acids; (2) the biterminal pathway, which produces dicarboxylic acids through oxidation at both ends; and (3) the subterminal pathway, in which oxidation at a subterminal carbon yields ester intermediates (Fuchs 1999; Izquierdo 2013). Despite considerable advances in understanding aerobic hydrocarbon degradation, the diversity of hydrocarbons and the variety of enzymatic systems employed by different microorganisms continue to complicate a complete understanding of these processes (Fuchs et al. 2011; Oosterkamp et al. 2015; Solís-González and Loza-Tavera 2019). To overcome these limitations, transcriptomic approaches have become valuable tools for elucidating the molecular mechanisms involved in hydrocarbon metabolism (Hong et al. 2016; Li, Huang, and Liu 2020).

To our knowledge, this study provides the first transcriptomic analysis of *B. licheniformis* M2-7 during gasoline oxidation. Previous transcriptomic studies involving hydrocarbon degradation have been conducted in *P. aeruginosa* strains N002, TP16, and J001, *Achromobacter* sp. HZ01, and *Lysinibacillus fusiformis*, revealing both similarities in the metabolic pathways activated and differences in the number of

297 DEGs, which ranged from 742 to 3,580 (Gunasekera et al. 2013; Hong et al. 2016; Li, Huang, and Liu
298 2020; Das et al. 2020). The transcriptional response observed in *B. licheniformis* M2-7 (Figs. 1 and 2)
299 resembles that reported for *P. aeruginosa* ATCC 33988 grown in jet fuel, in which 3,580 genes were
300 differentially expressed, including 2,963 upregulated and 617 downregulated genes (Gunasekera et al.
301 2013). Likewise, 742 DEGs (278 upregulated and 464 downregulated) were identified in *Achromobacter*
302 sp. HZ01 grown in an oil-containing medium (Hong et al. 2016), whereas *L. fusiformis* strain 15-4 exhibited
303 2,192 DEGs (1,312 upregulated and 880 downregulated) under petroleum exposure (Li, Huang, and Liu
304 2020). In *P. aeruginosa* strains N002, TP16, and J001, 81, 269, and 137 genes, respectively, were
305 differentially expressed in the presence of crude oil (Das et al. 2020). Similarly, transcriptomic analysis of
306 petroleum-contaminated soils supplemented with high nitrogen concentrations (1,360 mf N/kg) revealed
307 2,675 DEGs, including 974 upregulated and 1,701 downregulated genes, while achieving a 12.8% reduction
308 in hydrocarbon contamination (Ou et al. 2024).
309 The results of the pathway enrichment analysis (Fig. 3) are consistent with those reported for *P. aeruginosa*
310 ATCC 33988 grown in crude oil, in which pathways associated with membrane proteins, putative enzymes,
311 and transcriptional regulators were activated (Gunasekera et al., 2013). Similarly, in *Achromobacter* sp.
312 grown on alkanes, genes involved in amino acid transport and metabolism, energy production and
313 conversion, ABC transport systems, and fatty acid metabolism were identified (Hong et al., 2016). In
314 *Lysinibacillus fusiformis* strain 15-4 grown in petroleum, DEGs were associated with energy production
315 and conversion, cell wall/membrane/envelope biogenesis, transcriptional regulation, transport processes,
316 amino acid metabolism, carbohydrate metabolism, and ABC transporters (Li, Huang, and Liu 2020).
317 Previous studies have also shown that adaptation to hydrocarbon-rich environments involves changes in
318 cellular structures and biofilm formation. Gunasekera et al. (2017) identified a protein involved in cell
319 adhesion and biofilm formation that is essential for survival under hydrocarbon stress. In addition, genes
320 encoding efflux pumps, porins, extracellular polysaccharides, and biofilm-associated proteins are
321 upregulated when *P. aeruginosa* ATCC 33988 is exposed to fuel (Gunasekera et al. 2013). Likewise, the
322 *csrA* gene, which belongs to the carbon regulatory system, has been reported to be upregulated. A similar
323 response was observed in *B. licheniformis* M2-7 after 6 h of growth in minimal saline medium containing
324 0.1% gasoline, in which *csrA* expression increased approximately 2-fold relative to the basal condition
325 (Ángel et al. 2020).

Ángel et al. (2020) also reported that one of the responses of *B. licheniformis* M2-7 to glucose metabolism was the production of numerous peritrichous flagella. Although this was initially thought to promote motility in semisolid media, the authors proposed that the excessive number of flagellar structures might instead impair bacterial movement. This hypothesis is supported by the motility phenotype observed in the present study (Fig. 4), in which reduced motility was detected under gasoline oxidation conditions. Although few studies have specifically addressed gasoline catabolism, research on diesel degradation provides valuable insights. In *Alcanivorax dieselolei,* genes involved in *n*-hexadecane metabolism, including those encoding monooxygenases, cytochrome P450 oxidases, alcohol dehydrogenases, and aldehyde dehydrogenases, were upregulated at both the transcriptional and translational levels (Zining et al. 2023). Likewise, *Alcanivorax* sp. strain 24 grown in the presence of alkanes expressed two cytochrome P450 enzymes, three alkane monooxygenases (*AlkB*), and two enzymes involved in long-chain alkane degradation (Zadjelovic et al. 2020).

In the present study, genes associated with adaptation to oxygen limitation (*resE, resD*, and *ctaA*) were downregulated, whereas genes involved in the response to low temperatures (*desK* and *des*) were activated. This expression pattern may reflect the physiological characteristics of strain M2-7, whose optimum growth temperature is 50 °C. Therefore, incubation at 37 °C may represent a suboptimal or mildly stressful condition for this thermotolerant bacterium (Guevara-Luna et al. 2018). Another pathway affected by gasoline exposure was quorum sensing, which regulates the expression of the lichenysin synthetase genes (*lchAA, lchAB, lchAC,* and *lchAD*). Although these genes appeared to be upregulated in the RNA-seq analysis, RT-qPCR validation and biosurfactant quantification indicated reduced expression and lower biosurfactant production (Table 2; Fig. 5), suggesting that additional regulatory mechanisms may influence lichenysin synthesis. Biosurfactants produced by *Bacillus* species, including surfactins, fengycins, lichenysins, and bacillomycins, can emulsify hydrocarbons by reducing surface tension at the oil-water interface, thereby increasing the bioavailability of gasoline and diesel components (Kayath et al. 2019; Hoffmann et al. 2021; Okeke et al. 2022). Although these molecules are frequently considered important facilitators of hydrocarbon degradation, their role may vary depending on the metabolic state of the cells and the environmental conditions (Stancu 2020; Zambry et al. 2021).

Analysis of the affected metabolic modules enabled the reconstruction of a model for the degradation pathways used by *B. licheniformis* M2-7 during the oxidation of gasoline components (Fig. 6). The pathways involved in gasoline oxidation and carbon utilization were successfully predicted. The initial step

in the degradation of aromatic hydrocarbons appears to involve dioxygenase enzymes, which incorporate two oxygen atoms into the aromatic ring. This reaction requires the presence of molecular oxygen to initiate the enzymatic breakdown of aromatic compounds (Haddock 2010; Imron et al. 2020; Guevara-Luna et al. 2022).

These enzymes catalyze the incorporation of oxygen into the substrate, resulting in the hydroxylation of benzene and the formation of the less stable intermediate cis-benzene dihydrodiol. Cis-diol dehydrogenase subsequently converts this compound into catechol (Ukiwe et al. 2013; Imron and Tita 2018; Imron et al. 2020). The catechol ring is then cleaved by intradiol (ortho) or extradiol (meta) dioxygenases, leading to ring opening through the incorporation of oxygen molecules. Specifically, catechol 1,2-dioxygenase (intradiol dioxygenase) converts catechol into cis,cis-muconic acid, whereas catechol 2,3-dioxygenase (extradiol dioxygenase) converts catechol into 2-hydroxymuconic semialdehyde (Ukiwe et al. 2013; Imron and Tita 2018; Imron et al. 2020). Because the products generated are linear compounds, the resulting carboxylic acids and aldehydes are further metabolized through pathways similar to those involved in aliphatic hydrocarbon degradation. Acetyl-CoA produced during these reactions is subsequently generated through *β*-oxidation and enters central metabolic pathways, including the tricarboxylic acid cycle (Ukiwe et al. 2013; Imron and Tita 2018; Imron et al. 2020). Through these processes, hydrocarbon compounds are completely degraded and ATP is produced to support bacterial metabolism. Under aerobic conditions, CO_2 and H_2O are also generated as final byproducts (Ukiwe et al. 2013; Imron et al. 2020; Guevara-Luna et al. 2022). The proposed pathway was constructed based on BaP and pyrene, two of the most extensively studied PAHs and among the compounds for which the KEGG database provides the most comprehensive information. Both compounds have previously been investigated in *B. licheniformis* M2-7 (Guevara-Luna et al. 2018; Rojas-Aparicio et al. 2018; Guevara-Luna et al. 2022).

Conclusion

Transcriptomic analysis revealed that *B. licheniformis* M2-7 likely degrades gasoline through multiple metabolic pathways involving monooxygenases, reductases, dehydrogenases, and other catalytic enzymes associated with the metabolism of toxic compounds. The validation and characterization of a previously unannotated hypothetical protein also provided insight into its possible role in hydrocarbon catabolism, particularly in toluene degradation. These findings improve our understanding of the molecular mechanisms underlying gasoline oxidation by *B. licheniformis* M2-7 and highlight the potential of this strain for applications in bioremediation of ecosystems contaminated with petroleum-derived compounds.

Acknowledgements

This study was financially supported by the Secretaría de Ciencia, Humanidades, Tecnología e Innovación SECIHTI (Grant No. 746264)

References

IARC Working Group on the Evaluation of Carcinogenic Risks to Humans., & International Agency for Research on Cancer (1989) Diesel and gasoline engine exhausts and some nitroarenes.

Conceição PS de A, Cavalcanti, VL, Brandão JS, Ramos MF (2019) Prevention of occupational exposure to benzene at gas stations: actions of the Labor Inspection in Bahia, Brazil. Laborare 11(2):11-35. https://doi.org/10.33637/2595-847x.2019-26

Khan FI, Husain T, Hejazi R (2004) An overview and analysis of site remediation technologies. J of Environ Manage 71(2):95-122. https://doi.org/10.1016/j.jenvman.2004.02.003

WHO (2010) WHO guidelines for indoor air quality: selected pollutants. www.euro.who.int. Accessed 03 September 2025

Venny-Gan S, Ng HK (2012) Modified Fenton oxidation of polycyclic aromatic hydrocarbon (PAH)-contaminated soils and the potential of bioremediation as post-treatment. Science of the Total Environment 419:240-249. https://doi.org/10.1016/j.scitotenv.2011.12.053

Silva-Castro GA, Rodelas B, Perucha C, Laguna J, González-López J, Calvo C (2013) Bioremediation of diesel-polluted soil using biostimulation as post-treatment after oxidation with Fenton-like reagents: Assays in a pilot plant. Science of the Total Environment 445:347-355. https://doi.org/10.1016/j.scitotenv.2012.12.081

Khayati G, Barati M (2017) Bioremediation of Petroleum Hydrocarbon Contaminated Soil: Optimization Strategy Using Taguchi Design of Experimental (DOE) Methodology. Environmental Processes 4(2):451-461. https://doi.org/10.1007/s40710-017-0244-9

Elenga-Wilson PS, Kayath CA, Mokemiabeka NS, Nzaou SAE, Nguimbi E, Ahombo, G (2021) Profiling of Indigenous Biosurfactant-Producing *Bacillus* Isolates in the Bioremediation of Soil Contaminated by Petroleum Products and Olive Oil. Int J Microbiol 1-15. https://doi.org/10.1155/2021/9565930

Ugochukwu UC, Manning DAC, Fialips, CI (2014) Microbial degradation of crude oil hydrocarbons on organoclay minerals. J of Environ Manage 144:197-202. https://doi.org/10.1016/j.jenvman.2014.06.002

Sarkar J, Kazy SK, Gupta A, Dutta A, Mohapatra B, Roy A, Bera P, Mitra A, Sar P (2016) Biostimulation of indigenous microbial community for bioremediation of petroleum refinery sludge. Front. Microbiol. 7:1407. https://doi.org/10.3389/fmicb.2016.01407

Prosser CM, Redman AD, Prince RC, Paumen ML, Letinski DJ, Butler JD (2016) Evaluating persistence of petroleum hydrocarbons in aerobic aqueous media. Chemosphere 155:542-549. https://doi.org/10.1016/j.chemosphere.2016.04.089

Gupta G, Chandra A, Varjani SJ, Banerjee C, Kumar V (2018) Role of Biosurfactants in Enhancing the Microbial Degradation of Pyrene. Energy, Environment, and Sustainability, 375-386. https://doi.org/10.1007/978-981-10-7485-1_18

Ángel LIS, Segura D, Jiménez JT, Barrera MÁR, Pineda CO, Ramírez YR (2020) Carbon storage regulator A (*csrA*) gene regulates motility and growth of *Bacillus licheniformis* in the presence of hydrocarbons. Microbio Biotechnol Lett 48(2):185-192. https://doi.org/10.4014/mbl.1909.09014

Baburam C, Feto NA (2021) Mining of two novel aldehyde dehydrogenases (DHY-SC-VUT5 and DHY-G-VUT7) from metagenome of hydrocarbon contaminated soils. BMC Biotechnol 21(1). https://doi.org/10.1186/s12896-021-00677-8

Frantsuzova E, Delegan Y, Bogun A, Sokolova D, Nazina T (2023) Comparative Genomic Analysis of the Hydrocarbon-Oxidizing Dibenzothiophene-Desulfurizing *Gordonia* Strains. Microorganisms, 11(1). https://doi.org/10.3390/microorganisms11010004

Goma-Tchimbakala EJCD, Pietrini I, Goma-Tchimbakala J, Corgnati SP (2023) Use of Shotgun Metagenomics to Assess the Microbial Diversity and Hydrocarbons Degrading Functions of Auto-Mechanic Workshops Soils Polluted with Gasoline and Diesel Fuel. Microorganisms, 11(3):722. https://doi.org/10.3390/microorganisms11030722

Zhang S, Hu Z, Wang H (2019) Metagenomic analysis exhibited the co-metabolism of polycyclic aromatic hydrocarbons by bacterial community from estuarine sediment. Environ Int 129:308-319. https://doi.org/10.1016/j.envint.2019.05.028

Solís-González CJ, Loza-Tavera H (2019) *Alicycliphilus*: current knowledge and potential for bioremediation of xenobiotics. J Appl Microbiol 126(6):1643-1656. https://doi.org/10.1111/jam.14207

Guevara-Luna J, Alvarez-Fitz P, Ríos-Leal E, Acevedo-Quiroz M, Encarnación-Guevara S, Moreno-Godinez ME, Castellanos-Escamilla M, Toribio-Jiménez J, Romero-Ramírez Y (2018) Biotransformation

of benzo[a]pyrene by the thermophilic bacterium *Bacillus licheniformis* M2-7. World J Microbiol Biotechnol 34(7). https://doi.org/10.1007/s11274-018-2469-9

Guevara-Luna J, Serrano-Ángel LI, Rodrígez-Barrera MÁ, Hernández-Flores G, Toribio-Jiménez J, Toledo-Hernández E, Romero-Ramírez Y (2022) Isolated bacteria from hot springs able to use hydrocarbons as carbon source. Rev. Int. Contam. Ambient 38(3):68-77. https://doi.org/10.20937/RICA.54234

US EPA (1979) Annual Report to Congress. On Administartion of the Marine Protection, Research, and Sanctuaries.

Zhang Q, Davis LC, Erickson LE (1998) Effect of Vegetation on Transport of Groundwater and Non-aqueous Phase Liquid Contaminants. J Hazard Subst Res 1(1). https://doi.org/10.4148/1090-7025.1008

Lico D, Vuono D, Siciliano CB, Nagy J, de Luca P (2019) Removal of unleaded gasoline from water by multi-walled carbon nanotubes. J Environ Manage 237:636-643. https://doi.org/10.1016/j.jenvman.2019.02.062

Fuchs G (1999) Oxidation of organic compounds. In Biology of the Prokaryotes. JW Lengeler, G Drews, HG Schlegel, (eds.). Stuttgart: Thieme.

Izquierdo RA (2013) Biodegradación de HAPs durante la biorremediación aeróbica de suelos contaminados con hidrocarburos del petróleo. Análisis de poblaciones bacterianas y genes funcionales. Dissertation. Universitat de Barcelona.

Eskandari S, Hoodaji M, Tahmourespour A, Abdollahi A, Baghi T, Eslamian S, Ostad-Ali-Askari K (2017) Bioremediation of Polycyclic Aromatic Hydrocarbons by *Bacillus icheniformis* ATHE9 and *Bacillus mojavensis* ATHE13 as Newly Strains Isolated from Oil-Contaminated Soil. J Geogr Environ Earth Sci Int 11(2):1-11. https://doi.org/10.9734/jgeesi/2017/35447

Heitkamp MA, Freeman JP, Miller DW, Cerniglia CE (1988a) Pyrene Degradation by a *Mycobacterium* sp.: Identification of Ring Oxidation and Ring Fission Products. Appl Environ Microbiol 54(10). https://doi.org/10.1128/aem.54.10.2556-2565.1988

Heitkamp MA, Franklin W, Cerniglia CE (1988b) Microbial Metabolism of Polycyclic Aromatic Hydrocarbons: Isolation and Characterization of a Pyrene-Degrading Bacterium. Appl Environ Microbiol 54(10):2549-2555. https://doi.org/10.1128/aem.54.10.2549-2555.1988

Kelley I, Freeman JP, Cerniglia CE (1990) Identification of metabolites from degradation of naphthalene by a *Mycobacterium* sp. Biodegradation, 1(4):283-290. https://doi.org/10.1007/BF00119765

Stancu, MM (2020) Biosurfactant production by a *Bacillus megaterium* strain. Open Life Sci 15(1):629-637. https://doi.org/10.1515/biol-2020-0068

Zambry NS, Rusly MS, Awang NA, Md N, Yahya ARM (2021) Production of lipopeptide biosurfactant in batch and fed-batch *Streptomyces* sp. PBD-410L cultures growing on palm oil. Bioprocess Biosyst Eng 44(7):1577-1592. https://doi.org/10.1007/s00449-021-02543-5

Okeke ES, Okoye CO, Chidike-Ezeorba TP, Mao G, Chen Y, Xu H, Song C, Feng W, Wu X (2022) Emerging bio-dispersant and bioremediation technologies as environmentally friendly management responses toward marine oil spill: A comprehensive review. *J Environ Manag* 322:116-123. https://doi.org/10.1016/J.JENVMAN.2022.116123

Mata-Sandoval JC, Karns J, Torrents A (1999) High-performance liquid chromatography method for the characterization of rhamnolipid mixtures produced by *Pseudomonas aeruginosa* UG2 on corn oil. J Chromatogr A 864(2):211-220. https://doi.org/10.1016/s0021-9673(99)00979-6

Abalos A, Pinazo A, Infante MR, Casals M, García F, Manresa A (2001) Physicochemical and Antimicrobial Properties of New Rhamnolipids Produced by *Pseudomonas aeruginosa* AT10 from Soybean Oil Refinery Wastes. Langmuir ACS 17(5). http://doi.org/10.1021/la0011735

Gunasekera TS, Bowen LL, Zhou CE, Howard-Byerly SC, Foley WS, Striebich RC, Dugan LC, Ruiz ON (2017) Transcriptomic Analyses Elucidate Adaptive Differences of Closely Related Strains of *Pseudomonas aeruginosa* in Fuel. Appl Environ Microbiol 83(10):1-20. https://doi.org/10.1128/AEM

Rojas-Aparicio A, Hernández-Eligio JA, Toribio-Jiménez J, Rodríguez-Barrera M, Castellanos-Escamilla M, Romero-Ramírez Y (2018) Genetic expression of *poba* and *fabHB* in *Bacillus licheniformis* M2-7 in the presence of benzo[a]pyrene. Genet Mol Res 17(2). https://doi.org/10.4238/gmr16039916

Hong YH, Deng MC, Xu XM, Wu CF, Xiao X, Zhu Q, Sun XX, Zhou QZ, Peng J, Yuan JP, Wang JH (2016) Characterization of the transcriptome of *Achromobacter* sp. HZ01 with the outstanding hydrocarbon-degrading ability. Gene. 584(2):185-194. https://doi.org/10.1016/j.gene.2016.02.032

Li SW, Huang YX, Liu MY (2020) Transcriptome profiling reveals the molecular processes for survival of *Lysinibacillus fusiformis* strain 15-4 in petroleum environments. Ecotoxicol Environ Saf 192:110250. https://doi.org/10.1016/j.ecoenv.2020.110250

Das D, Mawlong GT, Sarki YN, Singh AK, Chikkaputtaiah C, Boruah HPD (2020) Transcriptome analysis of crude oil degrading *Pseudomonas aeruginosa* strains for identification of potential genes involved in crude oil degradation. Gene 755. https://doi.org/10.1016/j.gene.2020.144909

503 Zeinali M, Vossoughi M, Ardestani SK (2008) Naphthalene metabolism in *Nocardia otitidiscaviarum* strain
504 TSH1, a moderately thermophilic microorganism. Chemosphere 72(6):905-909.
505 https://doi.org/10.1016/j.chemosphere.2008.03.038
506 Chen S (2025) fastp 1.0: An ultra-fast all-round tool for FASTQ data quality control and preprocessing.
507 iMeta 4.5: e70078. https://doi.org/10.1002/imt2.70078.
508 Magoč T, Salzberg SL (2011) FLASH: fast length adjustment of short reads to improve genome assemblies.
509 Bioinformatics 27(21):2957–2963, https://doi.org/10.1093/bioinformatics/btr507
510 Prjibelski A, Antipov D, Meleshko D, Lapidus A, Korobeynikov A (2020) Using SPAdes De Novo
511 Assembler. Curr Protoc Bioinformatics 70(1). https://doi.org/10.1002/cpbi.102
512 Li H, Durbin R (2009) Fast and accurate short read alignment with Burrows-Wheeler Transform.
513 Bioinformatics 25(16):1754-60. https://doi.org/10.1093/bioinformatics/btp352
514 Danecek P, Bonfield JK, Liddle J, Marshall J, Ohan V, Pollard MO, Whitwham A, Keane T, McCarthy SA,
515 Davies RM, Li H (2021) Twelve years of SAMtools and BCFtools, GigaScience, 10(2).
516 https://doi.org/10.1093/gigascience/giab008
517 Trapnell C, Roberts A, Goff L, Pertea G, Kim D, Kelley DR, Pimentel H, Salzberg SL, Rinn JL, Pachter L
518 (2012) Differential gene and transcript expression analysis of RNA-seq experiments with TopHat and
519 Cufflinks. Nat Protoc 7:562-578. https://doi.org/10.1038/nprot.2012.016
520 Anders S, Huber W (2010) Differential expression analysis for sequence count data. Genome Biol 11(106).
521 https://doi.org/10.1186/gb-2010-11-10-r106
522 Ewels P, Peltzer A, Fillinger S, Patel H, Alneberg J, Wilm A, Garcia MU, Tommaso P & Nahnsen S (2020)
523 The nf-core framework for community-curated bioinformatics pipelines. Nat Biotechnol 38(3):276-278.
524 https://doi.org/10.1038/s41587-020-0439-x
525 Kanehisa M, Goto S (2000) KEGG: Kyoto Encyclopedia of Genes and Genomes. Nucleic Acids Res,
526 28(1):27-30. https://doi.org/10.1093/nar/28.1.27
527 Livak KJ, Schmittgen TD (2001) Analysis of relative gene expression data using real-time quantitative PCR
528 and the 2− CT Method. Methods, 25:402-408. https://doi.org/10.1006/meth.2001.1262
529 Sun W, Cao W, Jiang M, Saren G, Liu J, Cao J, Ali I, Yu X, Peng C, Naz I (2018) Isolation and
530 characterization of biosurfactant-producing and diesel oil degrading *Pseudomonas* sp. CQ2 from
531 Changqing oil field, China. RSC Adv 8(69):39710-39720. https://doi.org/10.1039/c8ra07721e

Agnez-Lima LF, Vainstein MH, Zhang X (2024) Editorial: Microbial hydrocarbon degradation and bioremediation: from genes to pathways. Front. Microbiol 15:1416516. https://doi.org/10.3389/fmicb.2024.1416516

Gunasekera TS, Striebich RC, Mueller SS, Strobel, EM, Ruiz ON (2013) Transcriptional profiling suggests that multiple metabolic adaptations are required for effective proliferation of *Pseudomonas aeruginosa* in jet fuel. Environ Sci Technol 47:13449-13458. https://doi.org/10.3389/fmicb.2024.1416516

Fuchs G, Boll M, Heider J (2011) Microbial degradation of aromatic compounds- From one strategy to four. Nat Rev Microbiol 9(11):803-816. https://doi.org/10.1038/nrmicro2652

Oosterkamp MJ, Boeren S, Atashgahi S, Plugge CM, Schaap PJ, Stams AJM (2015) Proteomic analysis of nitrate-dependent acetone degradation by *Alicycliphilus denitrificans* strain BC. FEMS Microbiol Lett 362(11). https://doi.org/10.1093/femsle/fnv080

Ou Y, Wu M, Yu Y, Liu Z, Kang H, Hu M, Zhang C, Chen X (2024) Influence Mechanisms Underlying the Degradation of Petroleum Hydrocarbons in Response to Various Nitrogen Dosages Supplementation Through Metatranscriptomics Analysis. J Hazard Mater 5(487):137074. https://doi.org/10.1016/j.jhazmat.2024.137074

Zining W, Guangshan W, Xiyan Z, Wanpeng W, Zongze S (2023) Regulation of alkane metabolism in *Alcanivorax* based on transcriptome and translatome. AMS 63(12):4606-4624. https://doi.org/10.13343/j.cnki.wsxb.20230268

Zadjelovic V, Gibson MI, Dorador C, Christie-Oleza JA (2020) Genome of *Alcanivorax* sp. 24: a hydrocarbon degrading bacterium isolated from marine plastic debris. Mar Genom 49:100686 https://doi.org/10.1016/j.margen.2019.05.001

Kayath CA, Ibala-Zamba A, Goma-Tchimbakala J, Mamonékéné V, Mombo Makanga GM, Lebonguy AA, Nguimbi E (2019) Microbiota landscape of gut system of guppy fish (*Poecilia reticulata*) plays an outstanding role in adaptation mechanisms. Int J Microbiol 2019:1-9. https://doi.org/10.1155/2019/3590584

Hoffmann M, Mück D, Grossmann L, Greiner L, Klausmann P, Henkel M, Lilge L, Weiss J, Hausmann R (2021) Surfactin from *Bacillus subtilis* displays promising characteristics as O/W-emulsifier for food formulations. Colloids Surf B Biointerfaces 203. https://doi.org/10.1016/j.colsurfb.2021.111749

Haddock JD (2010) Aerobic degradation of aromatic hydrocarbons: enzyme structures and catalytic mechanisms. Handbook Hydrocarb. Lipid Microbio 1058-1067. https://doi.org/10.1007/978-3-540-77587-4

Imron MF, Kurniawan SB, Ismail NI, Abdullah SRS (2020) Future challenges in diesel biodegradation by bacteria isolates: A review. J Clean Prod 251:119716. https://doi.org/10.1016/j.jclepro.2019

Ukiwe LN, Egereonu UU, Njoku PC, Nwoko CIA, Allinor JI (2013) Polycyclic aromatic hydrocarbons degradation techniques: a Review. Int J Chem 5(4):43-48. https://doi.org/10.5539/ijc.v5n4p43.

Imron MF, Titah HS (2018) Biodegradation of diesel by *Acinetobacter lwoffii* and *Vibrio alginolyticus* isolated from ship dismantling facility in Tanjungjati coast, Madura, Indonesia. JABS 12(1):1-8. https://jabsonline.org/index.php/jabs/article/view/553

Statements & Declarations

Funding

The authors declare that no funds, grants, or other support were received during the preparation of this manuscript.

Competing Interests

The authors have no relevant financial or non-financial interests to disclose, the corresponding author states that there is no conflict of interest.

Author Contributions

All authors contributed to the study conception and design. Material preparation, data collection and analysis were performed by Augusto Rojas-Aparicio, Mariana Reyes-Prieto, Alberto Hernández-Eligio, Jeiry Toribio-Jiménez and Yanet Romero Ramírez. The first draft of the manuscript was written by all authors. All authors read and approved of the final manuscript.

Ethical approval

This article does not contain any studies with human participants or animals performed by any of the authors.

Data Availability

The datasets generated during and/or analysed during the RNA-seq study are available in the NCBI Gene Expression Omnibus database under accession number GSE337535 (https://www.ncbi.nlm.nih.gov/geo/query/acc.cgi?acc=GSE337535).

Fig. 1 Bioinformatic analysis of RNA-seq data from *B. licheniformis* M2-7 under gasoline oxidation conditions. a) Quality assessment of control and treatment libraries performed using Fastp. Phred quality scores were used to evaluate sequencing quality. **b)** Distribution of differential abundance values. The counts of the 500 genes showing the greatest variation are presented, together with the standard deviation for each sample based on raw counts, normalized counts, and variance-stabilized counts. Control samples are shown in gray and gasoline-treated samples in orange. Points outside the whiskers represent genes with the highest variability. **c)** Dendrogram showing the 1,000 most variable genes across samples. Control samples supplemented with 2% glucose are indicated in gray, whereas samples treated with 0.1% gasoline are indicated in brown. Sample clustering was based on Spearman's correlation. **d)** Principal component analysis (PCA) of the RNA-seq data. The first two principal components (PC1 and PC2) together explain more than 80% of the total variance.

Fig. 2 Differential expression analysis of *B. licheniformis* M2-7 under gasoline oxidation conditions. The volcano plot illustrates the genes identified as differentially expressed by RNA-seq analysis between gasoline-treated and control cultures. Genes with a fold change greater than 2 are highlighted in orange. Downregulated genes are located on the left side of the plot, whereas upregulated genes are located on the right. Genes with a fold change of less than 2 are shown in gray. The horizontal dashed line indicates the significance threshold ($p < 0.05$).

Fig. 3 Enriched metabolic pathways in *B. licheniformis* M2-7 during gasoline oxidation. The bar graph shows the numbers of DEGs associated with the major metabolic pathways affected during gasoline oxidation. The scale represents the number of genes assigned to each annotated pathway.

Fig. 4 Motility phenotype of *B. licheniformis* M2-7 in MSM. **a)** Control culture supplemented with 2% glucose, showing the sliding growth characteristic of the genus *Bacillus*. **b)** Culture supplemented with 0.1% gasoline, showing a growth pattern different from that of the control, with reduced sliding motility. A t-test revealed a significant difference between treatments ($P = 0.0293$).

Fig. 5 Biosurfactant production by *B. licheniformis* M2-7 under different growth conditions. Biosurfactant concentrations are expressed in mg/L. Two independent experiments were conducted, and a statistically significant difference between the glucose and gasoline treatments was observed ($P = 0.0027$).

Fig. 6 Proposed degradation pathways of the major gasoline components in *B. licheniformis* M2-7. The pathways were reconstructed based on the KEGG database using functional protein orthologs. Genes encoding proteins annotated in KEGG are shown in black. Genes in *B. licheniformis* M2-7 that exhibited differential expression in the RNA-seq analysis are shown in red and green. Red indicates genes that were upregulated, whereas green indicates genes whose expression was validated by RT-qPCR. Genes marked with an asterisk are clustered and may be co-regulated during gasoline oxidation. Dotted lines represent a single reaction step in metabolite degradation, whereas solid lines indicate multiple intermediate reactions. These intermediate steps are not shown because the corresponding pathways have been well characterized.

625

626

627

628

629

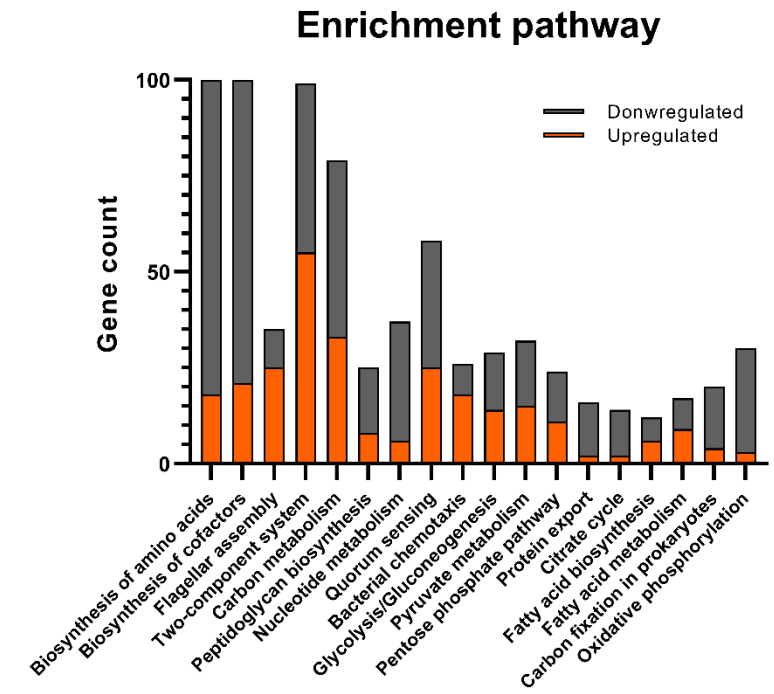
Enrichment pathway
Donwregulated
Upregulated
Gene count
100
50
0
Biosynthesis of amino acids
Biosynthesis of cofactors
Flagellar assembly
Two-component system
Carbon metabolism
Peptidoglycan biosynthesis
Nucleotide metabolism
Quorum sensing
Bacterial chemotaxis
Glycolysis/Gluconeogenesis
Pyruvate metabolism
Pentose phosphate pathway
Protein export
Citrate cycle
Fatty acid biosynthesis
Fatty acid metabolism
Carbon fixation in prokaryotes
Oxidative phosphorylation

630

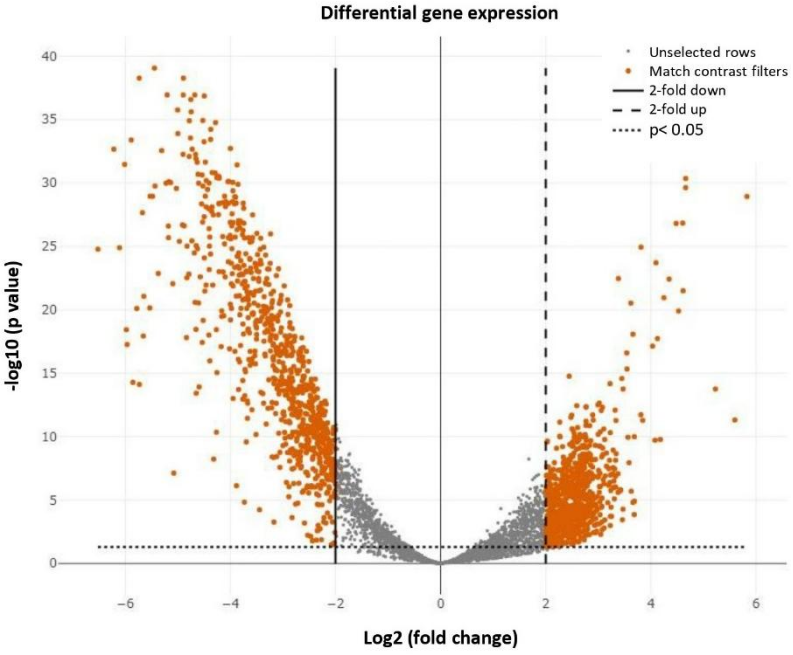
Differential gene expression
Unselected rows
Match contrast filters
2-fold down
2-fold up
p< 0.05
-log10 (p value)
40
35
30
25
20
15
10
5
0
−6
−4
−2
0
2
4
6
Log2 (fold change)

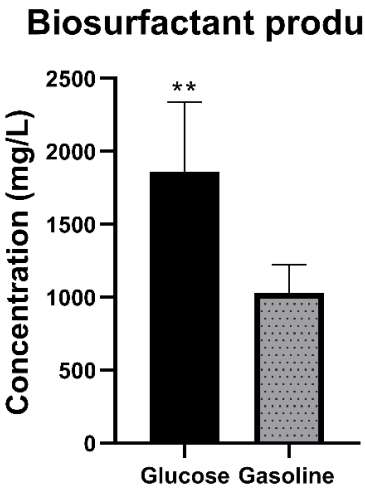

631

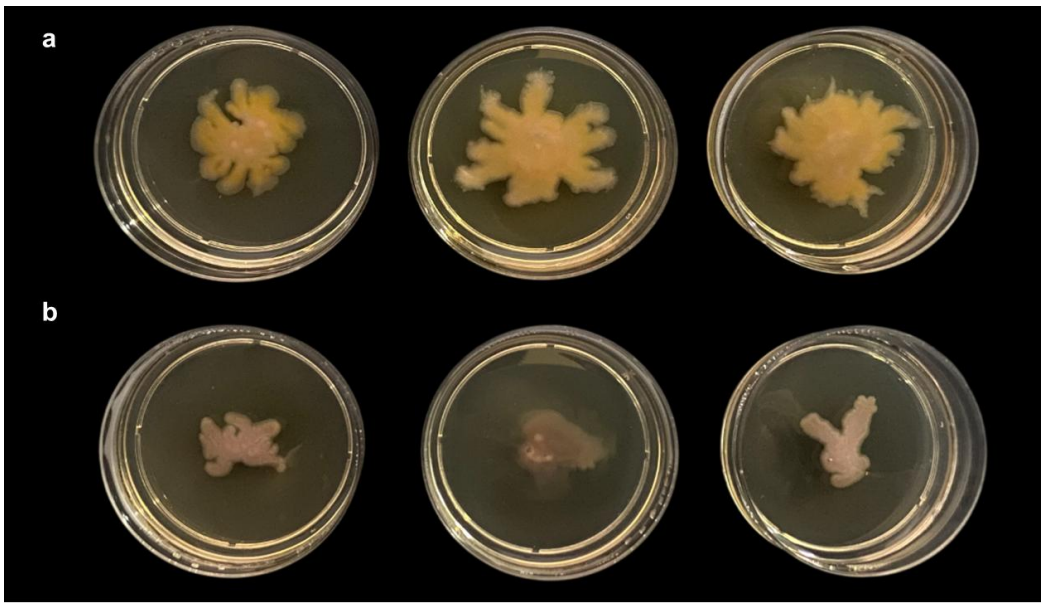

632

633

634

635

636

637

638

639

Table 1. DEGs in *B. licheniformis* M2-7 under gasoline oxidation conditions.

Locus ID	Gene annotation	Gene name	Log_2 FC	*P*-value
Upregulated genes identified by RNA-seq				
BLi00851	Acetoin dehydrogenase dihydrolipoamide-acetyltransferase E2 component AcoC	*acoC*	5.999	4.69E-33
BLi01955	YesF	*yesF*	5.358	1.92E-29
BLi04106	Transmembrane protein YxlE	*yxlE*	4.768	1.59E-29
BLi04015	YwdA	*ywdA*	4.754	1.09E-31
BLi01924	2-amino-3-ketobutyrate CoA ligase Kbl	*kbl*	4.743	3.52E-33
BLi04016	Sucrose-6-phosphate hydrolase SacA	*sacA1*	4.718	1.29E-26
BLi04108	Negative regulator YxlC	*yxlC*	4.691	2.56E-20
BLi00852	Acetoin dehydrogenase dihydrolipoamide dehydrogenase E3 component AcoL	*acoL*	4.551	1.56E-30
BLi05056	SR1-like protein	--	4.503	2.37E-21
BLi04105	Putative antimicrobial peptide ABC transporter ATP-binding protein YxlF	*yxlF*	4.463	1.71E-27
BLi02973	Putative phage protein	--	4.350	5.54E-44
BLi00495	Transketolase subunit A	--	4.310	5.34E-19
BLi02827	Levanase SacC	*sacC*	4.308	4.69E-23
BLi00494	Ascorbate-specific phosphotransferase system EIIC component UlaA	*ulaA*	4.206	3.17E-17
BLi02563	Glucomannan-specific phosphotransferase system EIIA component GmuA	*gmuA*	4.193	5.87E-09
BLi01143	Alpha-galactosidase MelA	*melA*	4.132	5.29E-28
BLi04107	Transmembrane protein YxlD	*yxlD*	4.116	1.35E-22
BLi02829	Fructose-specific phosphotransferase system EIIC component LevF	*levF*	4.022	1.12E-10
BLi00348	Putative antimicrobial peptide ABC exporter permease YclI	--	4.006	1.03E-15
BLi03464	Acyl-CoA dehydrogenase FadE	*fadE2*	3.983	7.02E-14
BLi01956	Hypothetical protein	--	5.999	6.29E-34
BLi04326	Hypothetical protein	--	2.184	9.00E-06
BLi04327	Putative acetyltransferase YycN	*yycN*	2.318	3.82E-05
BLi04328	Transmembrane protein	*ykvT*	3.982	2.21E-08
BLi01590	Putative cell wall hydrolase YkvT	*ykvU*	2.823	1.33E-09
BLi01591	Sporulation protein YkvU	*stoA*	2.280	2.54E-06
BLi01592	Thiol-disulfide oxidoreductase StoA	*zosA*	3.113	3.11E-08
				2.23E-07
BLi01695	Putative aromatic compound monooxygenase YhjG	*yhjG*	2.505	
BLi02016	Thiol-disulfide oxidoreductase ResA	*resA1*	2.357	5.27E-04
BLi02017	Putative manganese-containing catalase YdbD	*ydbD1*	2.058	1.29E-04

BLi02021	Putative transcriptional regulator	--	2.120	7.19E-05
BLi02023	Putative NAD(P)H nitroreductase MhqN	*mhqN*	2.608	1.74E-06
BLi02024	Putative ring-cleaving dioxygenase MhqO	*mhqO*	2.292	1.95E-08
BLi00401	Lichenysin synthase LchAA	--	1.120	3.12E-05
BLi00808	Putative pyridoxal phosphate-dependent aminotransferase	--	3.240	2.55E-08
BLi00809	Putative NAD(P)-dependent oxidoreductase YrbE	*yrbE*	2.765	5.90E-09
BLi00810	Nucleotide sugar dehydrogenase	--	2.589	1.22E-08
BLi03215	Cytochrome d ubiquinol oxidase subunit 1	*ythA*	3.134	4.85E-07
BLi03216	Cytochrome d ubiquinol oxidase subunit 2	*ythB*	3.351	2.39E-07
Downregulated genes identified by RNA-seq				
BLi00062	Putative septation protein SpoVG	*spoVG*	−7.239	9.00E-37
BLi03847	Acetolactate decarboxylase AlsD	*alsD*	−6.559	1.25E-12
BLi02085	Regulator ScdA	*scdA*	−5.926	8.63E-39
BLi01238	Transcriptional regulator Spx	*spx*	−5.895	6.39E-38
BLi01926	Putative regulator YmcA	*ymcA*	−4.982	1.52E-35
BLi00981	Putative two−component sensor histidine kinase	--	−4.671	1.37E-33
BLi01078	HTH-type transcriptional regulator ScoC	*scoC*	−3.996	8.34E-34
BLi01221	Beta-ketoacyl-acyl carrier protein synthase FabH	*fabH2*	−3.945	8.15E-26
BLi03360	Pleiotropic regulator DegQ	*degQ*	−3.614	5.71E-20
BLi03665	Glyceraldehyde-3-phosphate dehydrogenase 1	*gapA*	−6.191	6.96E-30
BLi00484	Assimilatory nitrite reductase NasD	*nasD*	−6.055	4.25E-53

640

Table 2. RT-qPCR validation of DEGs in *B. licheniformis* M2-7 under gasoline oxidation conditions.

Locus ID	Gene annotation	Gene name	Relative expression
Upregulated genes identified by RNA-seq			
BLi00851	Acetoin dehydrogenase dihydrolipoamide-acetyltransferase E2 component AcoC	*acoC*	7.01
BLi04105	Putative antimicrobial peptide ABC transporter ATP-binding protein YxlF	*yxlF*	9.78
BLi03464	Acyl-CoA dehydrogenase FadE	*fadE2*	452.26
BLi01956	Hypothetical protein	--	81.48
BLi04328	Transmembrane protein	*ykvT*	13.51
BLi01695	Putative aromatic compound monooxygenase YhjG	*yhjG*	8.41
BLi02024	Putative ring-cleaving dioxygenase MhqO	*mhqO*	34.07

BLi00809	Putative NAD(P)-dependent oxidoreductase YrbE	*yrbE*	6.59
BLi03215	Cytochrome d ubiquinol oxidase subunit 1	*ythA*	39.52
Downregulated genes identified by RNA-seq			
BLi00062	Putative septation protein SpoVG	*spoVG*	0.06
BLi00401	Lichenysin synthase LchAA	*lchAA*	0.54
BLi02085	Regulator ScdA	*scdA*	1.01
BLi03665	Glyceraldehyde-3-phosphate dehydrogenase 1	*gapA*	0.13
BLi01221	Beta-ketoacyl-acyl carrier protein synthase FabH	*fabH2*	0.03
BLi00484	Assimilatory nitrite reductase NasD	*nasD*	0.22
BLi03360	Pleiotropic regulator DegQ	*degQ*	0.001

n-fold changes were calculated based on the $2^{-\Delta\Delta CT}$ method (Livak and Schmittgen, 2001)

641

Supplementary Files

This is a list of supplementary files associated with this preprint. Click to download.

- SupplementaryTable1.docx
- Fig.6.Proposeddegradationpathways.tiff